

Pulsar Timing Response to Gravitational Waves with Spherical Wavefronts from a Massive Compact Source in the Quadrupole Approximation

RYOUSUKE KUBO,¹ KAKERU YAMAHIRA,¹ AND HIDEKI ASADA¹

¹ Graduate School of Science and Technology,
Hirosaki University,
3 Bunkyo-cho
Hirosaki, Aomori 036-8055, Japan

ABSTRACT

Pulsar timing arrays (PTAs) are searching for nanohertz-frequency gravitational waves (GWs) through cross-correlation of pulse arrival times from a set of radio pulsars. PTAs have relied upon a frequency-shift formula of the pulse, where planar GWs are usually assumed. Phase corrections due to the wavefront curvature have been recently discussed. In this paper, frequency-shift and timing-residual formulae are derived for GWs with fully spherical wavefronts from a compact source such as a binary of supermassive black holes, where the differences in the GW amplitude and direction between the Earth and the pulsar are examined in the quadrupole approximation. By using the new formulae, effects beyond the plane-wave approximation are discussed, and a galactic-center PTA as well as nearby GW source candidates are also mentioned.

Keywords: Gravitational waves (678); Pulsar timing method (1305); Gravitational wave astronomy (675); Millisecond pulsars (1062); Supermassive black hole (1663)

1. INTRODUCTION

The method of using radio pulse timing to search for gravitational waves (GWs) can be dated back to (Estabrook & Wahlquist 1975; Sazhin 1978; Detweiler 1979; Hellings & Downs 1983). A possible deviation from the expected noise has been reported by the NANOGrav team (Arzoumanian et al. 2020; Antoniadis 2022), and has been argued by several teams (Pol et al. 2021; Alam et al. 2021a,b; Arzoumanian et al. 2021a,b; Kaiser 2022; Goncharov et al. 2022). It is expected that the first detection by the International Pulsar Timing Array consortium may come soon (Castelvecchi 2022).

PTA studies have relied upon a frequency-shift formula of a radio pulse, where planar GWs are usually assumed (Estabrook & Wahlquist 1975; Detweiler 1979; Hellings & Downs 1983). The wavefront curvature for a distant GW source has been discussed as a correction; the Fresnel approximation is discussed (Deng & Finn 2011; McGrath & Creighton 2021). Toward PTA cosmology, the importance of distinguishing the comoving distance from the luminosity distance has been examined (D’Orazio & Loeb 2021; McGrath et al. 2022).

One may ask how a compact GW source affects PTA observational signatures. The main purpose of this paper is to discuss a PTA detector response to GWs from a

compact source such as binary supermassive black holes (SMBHs), which are thought to harbor in galactic centers. In section 2, we examine the pulse’s frequency shift and timing residual to GWs with fully spherical wavefronts from a compact source. In section 3, possible effects beyond the plane-wave approximation are discussed. Section 4 summarizes this paper. Throughout this paper, $c = 1$ and the Latin indices i, j run from 1 to 3.

2. PTA RESPONSE: FROM A PLANAR WAVE TO A SPHERICAL WAVE

2.1. PTA response to GWs

We begin with a derivation of the pulse’s frequency shift (Creighton & Anderson 2013; Maggiore 2018). In particular, we do not assume planar GWs such that our result can be applied also to GWs with spherical wavefronts as shown in next subsection.

We suppose that a radio pulse is emitted by a pulsar (P) at time t_P and arrives at the Earth (E) at t_E and position \mathbf{x}_E . The radio signal obeys the null condition as

$$0 = -dt^2 + (\delta_{ij} + h_{ij}^{TT})dx^i dx^j, \quad (1)$$

where the transverse and traceless (TT) gauge is used and h_{ij}^{TT} is GW perturbations. The unit vector along

the pulse is $dx^i/d\ell = -n_P^i$, where ℓ denotes the spatial length and n_P^i denotes the unit vector from E to P.

Eq. (1) is rearranged as

$$d\ell = \left(1 - \frac{1}{2}n_P^i n_P^j h_{ij}^{TT}(t, \mathbf{x}(t))\right) dt + O(h^2), \quad (2)$$

where $O(h^2)$ denotes the second order terms in h_{ij}^{TT} . In the TT gauge, the spatial coordinates of E and P are constants and the clocks on them are also aligned. See e.g. [Creighton et al. \(2009\)](#) for the role of the gauge in pulsar timing experiments.

The distance L between E and P is

$$\begin{aligned} L &= \int_P^E d\ell \\ &= t_E - t_P - \frac{1}{2}n_P^i n_P^j \int_{t_P}^{t_E} dt' h_{ij}^{TT}(t', \mathbf{x}(t')) \\ &\quad + O(h^2). \end{aligned} \quad (3)$$

It follows that $t_E = t_P + L + O(h)$.

The spatial position of the radio signal can be written at the lowest order as

$$\mathbf{x}(t) = \mathbf{x}_E + (t_P + L - t)\mathbf{n}_P + O(h). \quad (4)$$

Substituting Eq. (4) into Eq. (3) leads to

$$\begin{aligned} L &= t_E - t_P \\ &\quad - \frac{1}{2}n_P^i n_P^j \int_{t_P}^{t_P+L} dt' h_{ij}^{TT}(t', \mathbf{x}_E + (t_P - t' + L)\mathbf{n}_P) \\ &\quad + O(h^2). \end{aligned} \quad (5)$$

This agrees with e.g. Eq. (23.5) in [Maggiore \(2018\)](#).

For a radio pulse emitted at t_{em} and observed at t_{obs} , the notation change in Eq. (5) as $t_P \rightarrow t_{em}$ and $t_E \rightarrow t_{obs}$ leads to

$$\begin{aligned} L &= t_{obs} - t_{em} \\ &\quad - \frac{1}{2}n_P^i n_P^j \int_{t_{em}}^{t_{em}+L} dt' h_{ij}^{TT}(t', \mathbf{x}_E + (t_{em} - t' + L)\mathbf{n}_P) \\ &\quad + O(h^2). \end{aligned} \quad (6)$$

For the next pulse emitted at t'_{em} and observed at t'_{obs} ,

$$\begin{aligned} L &= t'_{obs} - t'_{em} \\ &\quad - \frac{1}{2}n_P^i n_P^j \int_{t'_{em}}^{t'_{em}+L} dt' h_{ij}^{TT}(t' + T_P, \mathbf{x}_E + (t_{em} - t' + L)\mathbf{n}_P) \\ &\quad + O(h^2). \end{aligned} \quad (7)$$

The linear perturbation by GWs suffices in the scope of this paper. Hence, $O(h^2)$ is omitted in the rest of this paper.

The observed period and intrinsic one of the radio pulse are $T_E = t'_{obs} - t_{obs}$ and $T_P = t'_{em} - t_{em}$, respectively. In the TT gauge, Eqs. (6) and (7) have the same separation L . Thereby, the deviation of the observed period from the intrinsic one is obtained as

$$\begin{aligned} \Delta T &\equiv T_E - T_P \\ &= \frac{1}{2}T_P n_P^i n_P^j \\ &\quad \times \int_{t'_{em}}^{t'_{em}+L} dt' \left[\frac{\partial}{\partial t'} h_{ij}^{TT}(t', \mathbf{x}) \right]_{\mathbf{x}=\mathbf{x}_E + (t_{em}-t'+L)\mathbf{n}_P}, \end{aligned} \quad (8)$$

where the GW period $T_{GW} \gg T_P \sim 1$ msec. is used.

The redshift due to the pulse period shift becomes

$$\begin{aligned} z &\equiv \frac{\Delta T}{T_P} \\ &= \frac{1}{2}n_P^i n_P^j \int_{t'_{em}}^{t'_{em}+L} dt' \left[\frac{\partial}{\partial t'} h_{ij}^{TT}(t', \mathbf{x}) \right]_{\mathbf{x}=\mathbf{x}_E + (t_{em}-t'+L)\mathbf{n}_P}. \end{aligned} \quad (9)$$

This causes the frequency shift of the radio signal as $\Delta f/f_E = -z$ because $f_E = 1/T_E$, $f_P = 1/T_P$ and $\Delta f \equiv f_E - f_P$. The partial differentiation $\partial/\partial t'$ acts only on the time argument in h_{ij}^{TT} but not on the spatial argument. Therefore, the integrand in Eq. (9) cannot be recast into a total differentiation, except for planar GWs. In a general situation without any approximation, therefore, we need perform the integral along the radio path.

2.2. Frequency shift by spherical wavefronts

Figure 1 shows a configuration of the Earth, a pulsar and a GW source (S). We suppose $\lambda_P \ll \lambda_{GW} < D \sim D_P$, where λ_P and λ_{GW} are wavelengths of the radio pulse and the GW, respectively.

In the quadrupole approximation, the GW at a radio pulse position $\mathbf{x}_R(t)$ is expressed as

$$h_{ij}^{TT}(t, \mathbf{x}_R(t)) = \frac{q_{ij}^{TT}(U, \mathbf{N}_R(t))}{|\mathbf{x}_R(t) - \mathbf{x}_S|}, \quad (10)$$

where q_{ij}^{TT} denotes the radiative part (the TT part of the second time derivative of the mass quadrupole moment multiplied by $2G$) of the GW source at \mathbf{x}_S and $U \equiv t - |\mathbf{x}_R(t) - \mathbf{x}_S|$ is the retarded time.

(7) We should note our treatment of the radio pulse position. In Eq. (10), q_{ij}^{TT} in its numerator causes the linear perturbation. In the linear approximation of Eq. (10), therefore, it suffices to use $\mathbf{x}_R(t) \equiv \mathbf{x}_E + (t_P + L - t)\mathbf{n}_P$ by safely ignoring $O(h)$ in Eq. (4).

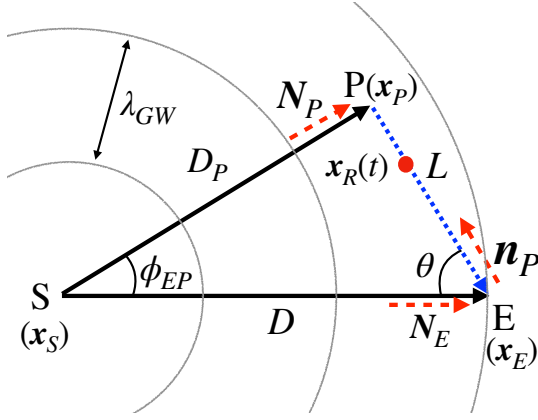


Figure 1. Configuration of the Earth (E), a pulsar (P) and a GW source (S). The black solid arrows denote GW paths to E or P, where red (in color) dashed arrows indicate the unit vectors along the GW propagation, \mathbf{N}_E and \mathbf{N}_P . The blue (in color) dotted arrow means the radio signal, where the unit vector from E to P is a red (in color) arrow \mathbf{n}_P . The distances between E and S, between E and P, and between P and S are D , L and D_P , respectively.

The GW propagation direction at R is

$$\mathbf{N}_R(t) \equiv \frac{\mathbf{x}_R(t) - \mathbf{x}_S}{|\mathbf{x}_R(t) - \mathbf{x}_S|}. \quad (11)$$

Note that q_{ij}^{TT} depends on $\mathbf{N}_R(t)$ via the TT projection operator, where $\mathbf{N}_R(t)$ as a function of time causes a deviation from a plane-wave case.

From Eq. (10), we obtain

$$\begin{aligned} & \left[\frac{\partial}{\partial t} h_{ij}^{TT}(t, \mathbf{x}) \right]_{\mathbf{x}=\mathbf{x}_R(t)} \\ &= \frac{1}{|\mathbf{x}_R(t) - \mathbf{x}_S|} \left[\frac{\partial q_{ij}^{TT}(U, \mathbf{N})}{\partial U} \right]_{\mathbf{N}=\mathbf{N}_R(t)}. \end{aligned} \quad (12)$$

We shall examine subtle calculations of the right-hand side of Eq. (12).

By direct calculations, we obtain

$$\begin{aligned} & \frac{d}{dt} q_{ij}^{TT}(U, \mathbf{N}_R(t)) \\ &= \frac{dU}{dt} \left[\frac{\partial q_{ij}^{TT}(U, \mathbf{N})}{\partial U} \right]_{\mathbf{N}=\mathbf{N}_R(t)} \\ &+ \frac{d\mathbf{N}_R(t)}{dt} \left[\frac{\partial q_{ij}^{TT}(U, \mathbf{N})}{\partial \mathbf{N}} \right]_{\mathbf{N}=\mathbf{N}_R(t)}, \end{aligned} \quad (13)$$

of which each term is calculated separately below.

First, we obtain

$$\frac{dU}{dt} = \frac{d}{dt} (t - |\mathbf{x}_R(t) - \mathbf{x}_S|)$$

$$\begin{aligned} &= 1 - \frac{d\mathbf{x}_R(t)}{dt} \cdot \frac{\mathbf{x}_R(t) - \mathbf{x}_S}{|\mathbf{x}_R(t) - \mathbf{x}_S|} \\ &= 1 + \mathbf{n}_P \cdot \mathbf{N}_R(t), \end{aligned} \quad (14)$$

where $d\mathbf{x}_R(t)/dt = -\mathbf{n}_P$ available from the time derivative of Eq. (4) is used in the third line.

Next, we find

$$\left[\frac{\partial q_{ij}^{TT}(U, \mathbf{N})}{\partial U} \right]_{\mathbf{N}=\mathbf{N}_R(t)} = O\left(\frac{q}{\lambda_{GW}}\right), \quad (15)$$

where q denotes the magnitude of $|q_{ij}^{TT}(U, \mathbf{N}_R(t))|$.

Thirdly,

$$\begin{aligned} \frac{d\mathbf{N}_R(t)}{dt} &= \frac{d}{dt} \frac{\mathbf{x}_R(t) - \mathbf{x}_S}{|\mathbf{x}_R(t) - \mathbf{x}_S|} \\ &= O\left(\frac{1}{D}\right), \end{aligned} \quad (16)$$

where we use $d\mathbf{x}_R(t)/dt = -\mathbf{n}_P = O(1)$ and $|\mathbf{x}_R(t) - \mathbf{x}_S| = O(D)$.

Finally, we obtain

$$\left[\frac{\partial q_{ij}^{TT}(U, \mathbf{N})}{\partial \mathbf{N}} \right]_{\mathbf{N}=\mathbf{N}_R(t)} = O(q). \quad (17)$$

From Eqs. (14)-(17), the second term in the right-hand side of Eq. (13) is smaller by factor of $O(\lambda_{GW}/D)$ than the first term. Therefore, Eq. (13) is rearranged as

$$\begin{aligned} & \frac{d}{dt} q_{ij}^{TT}(U, \mathbf{N}_R(t)) \\ &= (1 + \mathbf{n}_P \cdot \mathbf{N}_R(t)) \left[\frac{\partial q_{ij}^{TT}(U, \mathbf{N})}{\partial U} \right]_{\mathbf{N}=\mathbf{N}_R(t)} \left[1 + O\left(\frac{\lambda_{GW}}{D}\right) \right]. \end{aligned} \quad (18)$$

From Eq. (10), we obtain

$$\begin{aligned} \frac{d}{dt} h_{ij}^{TT}(t, \mathbf{x}_R(t)) &= \frac{1}{|\mathbf{x}_R(t) - \mathbf{x}_S|} \frac{d}{dt} q_{ij}^{TT}(U, \mathbf{N}_R(t)) \\ &+ q_{ij}^{TT}(U, \mathbf{N}_R(t)) \frac{d}{dt} \frac{1}{|\mathbf{x}_R(t) - \mathbf{x}_S|}. \end{aligned} \quad (19)$$

Here, we obtain

$$\frac{d}{dt} \frac{1}{|\mathbf{x}_R(t) - \mathbf{x}_S|} = O\left(\frac{1}{D^2}\right), \quad (20)$$

where $d\mathbf{x}_R(t)/dt = O(1)$ and $|\mathbf{x}_R(t) - \mathbf{x}_S| = O(D)$ are used again.

Note that a pulse trajectory is perturbed by GWs (Finn 2009), but the perturbation can induce terms of

$O(h/D)$ in Eq. (20), which cause only $O(h^2)$ in Eq. (19). Therefore, the perturbed trajectory can be ignored in the present paper.

From Eqs. (15), (18) and (20), the first term and second one in the right-hand side of Eq. (19) are $O(q/(D\lambda_{GW}))$ and $O(q/D^2)$, respectively. Namely, the first term is larger by factor of $O(D/\lambda_{GW})$ than the second one. We thus find

$$\begin{aligned} & \frac{d}{dt} h_{ij}^{TT}(t, \mathbf{x}_R(t)) \\ &= \frac{1}{|\mathbf{x}_R(t) - \mathbf{x}_S|} \frac{d}{dt} q_{ij}^{TT}(U, \mathbf{N}_R(t)) \left[1 + O\left(\frac{\lambda_{GW}}{D}\right) \right] \\ &= \frac{1 + \mathbf{n}_P \cdot \mathbf{N}_R(t)}{|\mathbf{x}_R(t) - \mathbf{x}_S|} \left[\frac{\partial q_{ij}^{TT}(U, \mathbf{N})}{\partial U} \right]_{\mathbf{N}=\mathbf{N}_R(t)} \left[1 + O\left(\frac{\lambda_{GW}}{D}\right) \right], \end{aligned}$$

where Eq. (18) is used in the third line.

From Eqs. (12) and (21), we obtain

$$\begin{aligned} & \frac{\partial}{\partial t} h_{ij}^{TT}(t, \mathbf{x}_R(t)) \\ &= \frac{1}{1 + \mathbf{n}_P \cdot \mathbf{N}_R(t)} \frac{d}{dt} h_{ij}^{TT}(t, \mathbf{x}_R(t)) \left[1 + O\left(\frac{\lambda_{GW}}{D}\right) \right] \\ &= \frac{d}{dt} \left(\frac{1}{1 + \mathbf{n}_P \cdot \mathbf{N}_R(t)} h_{ij}^{TT}(t, \mathbf{x}_R(t)) \right) \left[1 + O\left(\frac{\lambda_{GW}}{D}\right) \right], \end{aligned} \quad (22)$$

where we use in the last line

$$\frac{d}{dt} \frac{1}{1 + \mathbf{n}_P \cdot \mathbf{N}_R(t)} = O\left(\frac{1}{D}\right), \quad (23)$$

and $d(h_{ij}^{TT})/dt = O(h/\lambda_{GW})$.

Substituting Eq. (22) into Eq. (9) leads to

$$\begin{aligned} z &= \frac{1}{2} n_P^i n_P^j \\ &\times \int_{t'_{em}}^{t'_{em}+L} dt' \frac{d}{dt'} \left(\frac{1}{1 + \mathbf{n}_P \cdot \mathbf{N}_R(t')} h_{ij}^{TT}(t', \mathbf{x}_R(t')) \right) \\ &\times \left[1 + O\left(\frac{\lambda_{GW}}{D}\right) \right] \\ &= \frac{1}{2} n_P^i n_P^j \left[\frac{1}{1 + \mathbf{n}_P \cdot \mathbf{N}_E} h_{ij}^{TT}(t_E, \mathbf{x}_E) \right. \\ &\quad \left. - \frac{1}{1 + \mathbf{n}_P \cdot \mathbf{N}_P} h_{ij}^{TT}(t_P, \mathbf{x}_P) \right] \\ &\quad + O\left(\frac{h\lambda_{GW}}{D}\right), \end{aligned} \quad (24)$$

where the remainder term is $\sim 10^{-7}(\lambda_{GW}/10\text{pc})(100\text{Mpc}/D) \times O(h)$ and hence it can be safely ignored. The plane-wave formula is recovered by Eq. (24) in the limit $L/D \rightarrow 0$

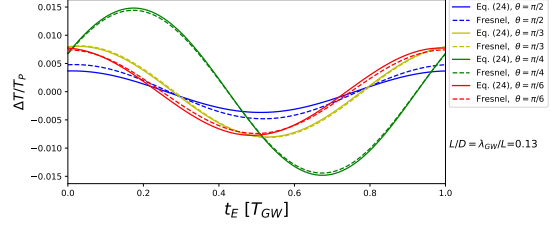


Figure 2. Redshift in PTA due to GWs from an edge-on circular binary. The vertical axis denotes the redshift $z = \Delta T/T_P$. The horizontal axis denotes t_E in the unit of T_{GW} . The colored dotted curves include only the phase correction by the Fresnel model (McGrath & Creighton 2021). The colored solid curves take account of also the GW amplitude and direction corrections via Eq. (24). For the curves to be recognized by eye, $L/D = \lambda_{GW}/L = 0.13$ is chosen.

(21) for which $\mathbf{N}_P \rightarrow \mathbf{N}_E$. Because of the retardation in Eq. (10), $h_{ij}^{TT}(t_E, \mathbf{x}_E)$ and $h_{ij}^{TT}(t_P, \mathbf{x}_P)$ come from the quadrupole moments at the GW source time $t_E - D$ and $t_P - D_P$, respectively, where $t_P = t_E - L$.

If we assumed $\mathbf{N}_E = \mathbf{N}_P$, $D = D_P$ and $\lambda_{GW} < L$, Eq. (24) could recover the wavefront-curvature effects in the literature (Deng & Finn 2011; McGrath & Creighton 2021; D’Orazio & Loeb 2021), where $\mathbf{N}_E = \mathbf{N}_P$ and $D = D_P$ are approximations for $L \ll D$, because $|\mathbf{N}_E - \mathbf{N}_P| = O(L/D)$.

2.3. Pulsar timing residual by spherical wavefronts

Finally, we mention the pulsar timing residual induced by the GWs, which is the integrated fractional period shift over the observation time (Creighton & Anderson 2013; Maggiore 2018; McGrath & Creighton 2021). The timing residual is

$$\text{Res}(t_{obs}) = \int_0^{t_{obs}} dt_E \frac{\Delta T}{T_P}, \quad (25)$$

where the initial time of the observation of interest is chosen as $t_E = 0$ without loss of generality and the observation time is $t_E = t_{obs}$.

By substituting Eq. (24) into Eq. (25), we obtain

$$\begin{aligned} & \text{Res}(t_{obs}) \\ &= \frac{1}{2} n_P^i n_P^j \left[\frac{1}{1 + \mathbf{n}_P \cdot \mathbf{N}_E} \int_0^{t_{obs}} dt_E h_{ij}^{TT}(t_E, \mathbf{x}_E) \right. \\ &\quad \left. - \frac{1}{1 + \mathbf{n}_P \cdot \mathbf{N}_P} \int_0^{t_{obs}} dt_E h_{ij}^{TT}(t_E - L, \mathbf{x}_P) \right] \\ &\quad + O\left(\frac{h(\lambda_{GW})^2}{D}\right), \end{aligned} \quad (26)$$

where $t_P = t_E - L$ is used in the third line, and $\int dt O(h\lambda_{GW}/D) \sim \int dt O(q_{ij}^{TT} \lambda_{GW}/D^2) \sim O(q_{ij}^{TT} (\lambda_{GW})^2/D^2) \sim O(h(\lambda_{GW})^2/D)$ (due to $\int dt q_{ij}^{TT} \sim \lambda_{GW} q_{ij}^{TT}$) is used in the last line.

The integral in the timing residual is dependent strongly on the GW waveform of concern. It cannot be always reduced to a compact form.

For its simplicity, let us consider a monochromatic GW regime as

$$h_{ij}^{TT}(t, \mathbf{x}) = A_{ij}^{TT}(\mathbf{x}) \exp \left[i \left(\frac{2\pi U}{\lambda_{GW}} \right) \right], \quad (27)$$

where the GW chirp is ignored. Then, the timing residual is expressed compactly as

$$\begin{aligned} \text{Res}(t_{obs}) &= \frac{i\lambda_{GW} n_P^i n_P^j}{4\pi} \\ &\times \left[\frac{A_{ij}^{TT}(\mathbf{x}_E)}{1 + \mathbf{n}_P \cdot \mathbf{N}_E} \left\{ \exp \left[-i \left(\frac{2\pi D}{\lambda_{GW}} \right) \right] \right. \right. \\ &\quad \left. \left. - \exp \left[i \left(\frac{2\pi(t_{obs} - D)}{\lambda_{GW}} \right) \right] \right\} \right. \\ &\quad \left. - \frac{A_{ij}^{TT}(\mathbf{x}_P)}{1 + \mathbf{n}_P \cdot \mathbf{N}_P} \left\{ \exp \left[-i \left(\frac{2\pi(L + D_P)}{\lambda_{GW}} \right) \right] \right. \right. \\ &\quad \left. \left. - \exp \left[i \left(\frac{2\pi(t_{obs} - L - D_P)}{\lambda_{GW}} \right) \right] \right\} \right] \\ &+ O \left(\frac{h(\lambda_{GW})^2}{D} \right). \end{aligned} \quad (28)$$

3. BEYOND THE PLANE-WAVE APPROXIMATION

3.1. Fresnel and L/D corrections

In addition to the Fresnel correction in the phase, there exist two other corrections. One correction comes from the distance difference, causing the GW amplitude difference between E and P. The fractional difference between paths SE and SP is $O(L/D)$ if $L < D$. The other correction is due to the difference in GW directions at E and P, namely the angle ϕ_{EP} between \mathbf{N}_E and \mathbf{N}_P , which satisfies

$$\begin{aligned} \sin \phi_{EP} &= \frac{L \sin \theta}{\sqrt{D^2 + L^2 - 2DL \cos \theta}} \\ &= \frac{L}{D} \cos \theta + O \left(\frac{L^2}{D^2} \right), \end{aligned} \quad (29)$$

where the cosine formula is used for the triangle EPS and the second equality holds only for $L < D$. The two next-leading corrections are thus $O(L/D)$.

As an illustration, let us examine the fourth exponential function in Eq. (28). It is expanded in the Fresnel approximation (McGrath & Creighton 2021; McGrath et al. 2022) as

$$\exp \left[i \left(\frac{2\pi(t_{obs} - L - D_P)}{\lambda_{GW}} \right) \right]$$

$$\begin{aligned} &= \left[1 + \frac{i\pi(1 - \cos^2 \theta)L^2}{D\lambda_{GW}} + O \left(\frac{L^4}{D^2(\lambda_{GW})^2} \right) \right] \\ &\times \exp \left[i \left(\frac{2\pi(t_{obs} - D - L(1 - \cos \theta))}{\lambda_{GW}} \right) \right], \end{aligned} \quad (30)$$

where $D_P = (D^2 - 2DL \cos \theta + L^2)^{1/2}$ is expanded in L/D . The argument of the exponential function in the right-hand side of Eq. (30) corresponds to the phase in the plane wave approximation, and the second term in front of this function can be interpreted as the Fresnel correction of $O(L^2/(D\lambda_{GW}))$ (McGrath & Creighton 2021; McGrath et al. 2022).

Therefore, the Fresnel correction is still dominant in the timing residual also for a fully spherical wavefront, whereas corrections at $O(L/D)$ are next-leading, because $L > \lambda_{GW}$ for a typical PTA range. These scalings in the timing residual are consistent with those for the frequency shift as suggested by Eq. (24) and Figure 2.

3.2. Estimating the scaling of the corrections

For nearby cases, we make a comparison of the amplitude and direction corrections at $O(L/D)$ to the Fresnel phase correction at $O(L^2/(\lambda_{GW}D))$ (Deng & Finn 2011; McGrath & Creighton 2021; D’Orazio & Loeb 2021; Guo et al. 2022). For $\lambda_{GW} \ll L$, the former must be smaller than the latter. The ratio between them is $\sim 0.03(\lambda_{GW}/30\text{pc})(1\text{kpc}/L)$ for a millisecond pulsar at $L \sim 1$ kpc. For most of known millisecond pulsars, the L/D correction is thus smaller by two or more digits than the Fresnel correction.

One may ask if corrections of $O(L/D)$ can be comparable to the Fresnel one. The nearest millisecond pulsar J0437-4517 is located at $L = 156$ pc (Deller 2008), for which the ratio is $\sim 0.2(\lambda_{GW}/30\text{pc})(156\text{pc}/L)$ and hence the amplitude and direction corrections are comparable to the Fresnel correction. For this case, however, all of these corrections are negligible.

3.3. On nearby GW source candidates

Once future observations in PTAs detect a GW signal, one may ask if the plane-wave ansatz is sufficient for the PTA data. The corrections at $O(L/D)$ are less than roughly 10^{-3} for $L \sim 10$ kpc and $D > 10$ Mpc, for which the distance correction is ~ 0.1 percents or less. Recent PTA bounds on SMBHs within about 500 Mpc (Arzoumanian et al. 2021a), most of targeted galaxies are distant (> 10 Mpc). However, a few of them are near. For instance, J00424433+4116074 is a galaxy at 0.82 Mpc, for which effects beyond plane waves, especially the Fresnel effect, may reach one percent or more. In PTA data analysis for galaxies within $D \sim 100$ kpc in the local group, the effects can be ten percents or more, and hence they should be considered.

The corrections can be more important for nearer GW sources. The existence of a binary of SMBHs in M31 is suggested (Lauer et al. 1993; Bender et al. 2005). For such a nearby case, L/D is $\sim 10^{-2}$, for which the corrections can be at the several percent level.

3.4. Galactic-center PTA

There could exist a hidden companion to Sagittarius A* (Sgr A*). It has been recently discussed that the Sgr A* observations combined with dynamical stability argument seem to rule out a $10^5 M_\odot$ companion (Naoz et al. 2020). Even with the companion with $\sim 10^5 M_\odot$ and the orbital radius of ~ 100 AU, it is expected to be below the typical PTA sensitivity, which usually assumes $D_P \sim 10$ kpc for a galactic center source.

Yet, a large population of pulsars is expected to reside in the galactic center (Pfahl & Loeb 2004). In particular, recent analyses of the gamma-ray emission excess using the entire Fermi data support that the excess at the galactic center can be caused by a population of thousands of undetected millisecond pulsars (Ajello et al. 2016; Bartels et al. 2016; Calore et al. 2016; Lee et al. 2016; Gonthier et al. 2018). The first pulsar survey in the galactic center at short millimeter wavelengths, using several frequency bands between 84 and 156 GHz, has been done, and it has demonstrated that surveys at extremely high radio frequencies are capable of discovering new pulsars (Torne et al. 2021). The survey at a low frequency of ~ 310 MHz has been also done (Hyman et al. 2019).

Along this direction, an interesting possibility has been argued that PTAs using millisecond pulsars within 0.1-1 pc to Sgr A* can probe intermediate-mass BHs (IMBHs) (Kocsis et al. 2012), where the plane-wave formulae are used.

Let us suppose a hypothetical IMBH with $\sim 10^4 M_\odot$ orbiting around Sgr A* with the orbital radius $a \sim 100$ AU, for which the typical GW period is ~ 1 year. For instance, we assume a hypothetical pulsar at ~ 10 pc from the galactic center. This distance is more likely than the speculative value of 0.1 pc in Kocsis et al. (2012). The amplitude of GWs at the position of the pulsar is $h \sim ma^2/(D_P(T_{GW})^2) \sim Mm/(D_P a) \sim 10^{-14}(M/(10^6 M_\odot))(m/(10^4 M_\odot))(10 \text{ pc}/D_P)(100 \text{ AU}/a)$, where M and m are the mass of Sgr A* and that of the IMBH, respectively.

For this hypothetical GW source, we shall make an order-of-magnitude estimate of the Earth term and the pulsar term in the timing residual. By using Eq. (30), these terms are roughly estimated as $\text{Res}(t_{obs})|_P \sim 10^{-6}(h_P/10^{-14})(\lambda_{GW}/1 \text{ pc})\text{sec.}$ and $\text{Res}(t_{obs})|_E \sim 10^{-9}(h_E/10^{-17})(\lambda_{GW}/1 \text{ pc})\text{sec.}$, where

h_P and h_E denote the GW strain at the pulsar and the Earth, respectively and $D = 10$ kpc, $D_P = 10$ pc, $\lambda_{GW} = 1$ pc are assumed. The Earth term in the timing residual is smaller by $D_P/D \sim 10^{-3}$ than the pulsar term.

Therefore, the Earth term in Eqs. (24) and (26) can be ignored practically for the galactic center PTA case that $D \sim L \sim 10 \text{ kpc} \gg D_P \sim 10 \text{ pc} > \lambda_{GW} \sim 1 \text{ pc}$, for which Eqs. (24) and (26) are still valid since $D_P > L$ is not assumed in the derivation of them. Note that expansions in L/D_P do not work for this system.

See also Guo et al. (2022) for the detectability of possible nearby GW sources by the Square Kilometer Array PTA, in which the GW direction and amplitude as well as the retarded time are considered in a fully numerical manner based on Eq. (1) of their paper for the frequency shift and Eqs. (6) and (7) for the antenna pattern functions. Although these equations apparently follow the equations in Anholm et al. (2009) based on plane waveforms, integral forms are used in their numerical computations for near fields (Guo et al. 2022), where they do not adopt the far-field approximation.

Finally, we mention another potentially useful application. It is beam-like GWs (Baral et al. 2020), for which the wavefront curvature can be significant even for a distant GW source. However, a generation mechanism of beam-like GWs is speculative.

4. SUMMARY

The frequency-shift and timing-residual formulae were derived for GWs with fully spherical wavefronts from a compact source. We confirmed that the Fresnel correction is a leading one under assumptions. As a next-leading correction, both the GW amplitude and direction corrections are at $O(L/D)$. A possible relation of nearby GW source candidates to the new formula was also mentioned. It is left for future to investigate the present formula for a larger parameter space in a more general situation.

We are grateful to Jolien Creighton, Casey McGrath, and Xiao Guo for the useful comments on the earlier version of the manuscript. We wish to thank Yu-uiti Sendouda and Ryuichi Takahashi for fruitful conversations. We thank Tatsuya Sasaki and Kohei Yamauchi for useful discussions. This work was supported in part by Japan Society for the Promotion of Science (JSPS) Grant-in-Aid for Scientific Research, No. 20K03963 (H.A.), in part by Ministry of Education, Culture, Sports, Science, and Technology, No. 17H06359 (H.A.).

REFERENCES

- Ajello, M., Albert, A., Atwood, W. B., et al. 2016, *ApJ*, 819, 44. doi:10.3847/0004-637X/819/1/44
- Alam, M. F., Arzoumanian, Z., Baker, P. T., et al. 2021, *ApJS*, 252, 4. doi:10.3847/1538-4365/abc6a0
- Alam, M. F., Arzoumanian, Z., Baker, P. T., et al. 2021, *ApJS*, 252, 5. doi:10.3847/1538-4365/abc6a1
- Anholm, M., Ballmer, S., Creighton, J. D. E., et al. 2009, *PhRvD*, 79, 084030. doi:10.1103/PhysRevD.79.084030
- Antoniadis, J., Arzoumanian, Z., Babak, S., et al. 2022, *MNRAS*, 510, 4873. doi:10.1093/mnras/stab3418
- Arzoumanian, Z., Baker, P. T., Blumer, H., et al. 2020, *ApJL*, 905, L34. doi:10.3847/2041-8213/abd401
- Arzoumanian, Z., Baker, P. T., Brazier, A., et al. 2021, *ApJ*, 914, 121. doi:10.3847/1538-4357/abfcd3
- Arzoumanian, Z., Baker, P. T., Blumer, H., et al. 2021, *PhRvL*, 127, 251302. doi:10.1103/PhysRevLett.127.251302
- Baral, P., Ray, A., Koley, R., et al. 2020, *European Physical Journal C*, 80, 326. doi:10.1140/epjc/s10052-020-7881-2
- Bartels, R., Krishnamurthy, S., & Weniger, C. 2016, *PhRvL*, 116, 051102. doi:10.1103/PhysRevLett.116.051102
- Bender, R., Kormendy, J., Bower, G., et al. 2005, *ApJ*, 631, 280. doi:10.1086/432434
- Calore, F., Di Mauro, M., Donato, F., et al. 2016, *ApJ*, 827, 143. doi:10.3847/0004-637X/827/2/143
- Castelvecchi, D. 2022, *Nature*, 602, 194. doi:10.1038/d41586-022-00170-y
- Creighton, T., Jenet, F. A., & Price, R. H. 2009, *ApJ*, 693, 1113. doi:10.1088/0004-637X/693/2/1113
- Creighton, J. D. E. & Anderson, W. G. 2013, *Gravitational-Wave Physics and Astronomy: An Introduction to Theory*, (Wiley, NY).
- Deller, A. T., Verbiest, J. P. W., Tingay, S. J. & Bailes, M. 2008, *ApJL*, 685, L67. doi:10.1086/592401
- Deng, X. & Finn, L. S. 2011, *MNRAS*, 414, 50. doi:10.1111/j.1365-2966.2010.17913.x
- Detweiler, S. 1979, *ApJ*, 234, 1100. doi:10.1086/157593
- D’Orazio, D. J. & Loeb, A. 2021, *PhRvD*, 104, 063015. doi:10.1103/PhysRevD.104.063015
- Estabrook, F. B. & Wahlquist, H. D. 1975, *General Relativ. Grav.*, 6, 439. doi:10.1007/BF00762449
- Finn, L. S. 2009, *PhRvD*, 79, 022002. doi:10.1103/PhysRevD.79.022002
- Goncharov, B., Thrane, E., Shannon, R. M., et al. 2022, *ApJL*, 932, L22. doi:10.3847/2041-8213/ac76bb
- Gonthier, P. L., Harding, A. K., Ferrara, E. C., et al. 2018, *ApJ*, 863, 199. doi:10.3847/1538-4357/aad08d
- Guo, X., Lu, Y., & Yu, Q. 2022, *ApJ*, 939, 55. doi:10.3847/1538-4357/ac9131
- Hyman, S. D., Frail, D. A., Deneva, J. S., et al. 2019, *ApJ*, 876, 20. doi:10.3847/1538-4357/ab11c8
- Hellings, R. W. & Downs, G. S. 1983, *ApJL*, 265, L39. doi:10.1086/183954
- Kaiser, A. R., Pol, N. S., McLaughlin, M. A., et al. 2022, *arXiv:2208.02307*
- Kocsis, B., Ray, A., & Portegies Zwart, S. 2012, *ApJ*, 752, 67. doi:10.1088/0004-637X/752/1/67
- Lauer, T. R., Faber, S. M., Groth, E. J., et al. 1993, *AJ*, 106, 1436. doi:10.1086/116737
- Lee, S. K., Lisanti, M., Safdi, B. R., et al. 2016, *PhRvL*, 116, 051103. doi:10.1103/PhysRevLett.116.051103
- Maggiore, M. 2018, *Gravitational Waves: Astrophysics and Cosmology* (Oxford Univ. Press, UK).
- McGrath, C. & Creighton, J. 2021, *MNRAS*, 505, 4531. doi:10.1093/mnras/stab1417
- McGrath, C., D’Orazio, D. J. & Creighton, J. 2022, *MNRAS*, 517, 1242. doi:10.1093/mnras/stac2593
- Naoz, S., Will, C. M., Ramirez-Ruiz, E., et al. 2020, *ApJL*, 888, L8. doi:10.3847/2041-8213/ab5e3b
- Pfahl, E. & Loeb, A. 2004, *ApJ*, 615, 253. doi:10.1086/423975
- Pol, N. S., Taylor, S. R., Kelley, L. Z., et al. 2021, *ApJL*, 911, L34. doi:10.3847/2041-8213/abf2c9
- Sazhin, M. V. 1978, *Soviet Ast.*, 22, 36.
- Torne, P., Desvignes, G., Eatough, R. P., et al. 2021, *A&A*, 650, A95. doi:10.1051/0004-6361/202140775